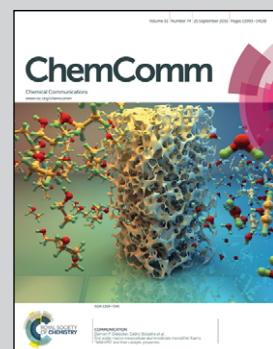


Showcasing research from A/Prof. Anthony O'Mullane's laboratory, School of Chemistry, Physics and Mechanical Engineering, Queensland University of Technology, Australia.

Generation of catalytically active materials from a liquid metal precursor

Exposing the liquid metal galinstan (GaInSn) to alkaline or reducing conditions results in the formation of In:Sn rich microspheres with a reduced Ga content. These microspheres are catalytically active for a versatile range of electron transfer reactions including ferricyanide, nitrophenol and Cr(vi) ion reduction.

As featured in:



See Anthony P. O'Mullane et al., *Chem. Commun.*, 2015, **51**, 14026.



Cite this: *Chem. Commun.*, 2015, 51, 14026

Received 26th June 2015,
Accepted 29th July 2015

DOI: 10.1039/c5cc05246g

www.rsc.org/chemcomm

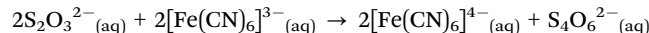
A facile route to prepare catalytically active materials from a galinstan liquid metal alloy is introduced. Sonicating liquid galinstan in alkaline solution or treating it in reducing media results in the creation of solid In/Sn rich microspheres that show catalytic activity toward both potassium ferricyanide and 4-nitrophenol reduction.

Liquid metals such as eutectic alloys of gallium and in particular Galinstan, an alloy of 68.5% gallium, 21.5% indium and 10.0% tin, have received significant attention thanks to their intriguing chemical and physical properties that make them amenable to applications in soft electronics,¹ pumps with no moving parts,² circuitry for stretchable devices,³ coolants,⁴ plasmonics,⁵ heavy metal ion sensors⁶ and MEMS devices.⁷ However, there has been burgeoning interest in modifying liquid metals to further increase their applicability by generating micro and nanosized liquid metal droplets⁸ combined with surface modification with semiconducting nanoparticles for use in actuating devices⁹ and photocatalysis.¹⁰ For many of these applications the presence of the native oxide on the surface is particularly critical to their operation.

In comparison to the field of liquid metals, the area of catalysis is significantly more mature and nanomaterials of various size, shape and composition have been extensively studied.¹¹ It has been reported that bimetallic or even trimetallic nanomaterials demonstrate increased activity over their individual metal components due to synergistic effects¹² and that the composition may be tuned for the specific reaction of interest. These nanomaterials

can either be employed as colloidal solutions that are subsequently removed after the reaction by sedimentation,¹³ immobilized within high surface area supports¹⁴ or indeed electrochemically generated as high surface area films adhered to a flat support,¹⁵ while each have their own limitations and advantages. However, the idea of investigating a liquid metal for its catalytic properties has yet to be reported. Therefore in this work we address this issue and investigate liquid metal galinstan for its catalytic activity towards model as well as commercially applicable reactions such as the reduction of ferricyanide ions and nitrophenol at room temperature. We demonstrate in this proof of concept that galinstan in fact acts as a precursor to a more reactive material of different composition that demonstrates activity towards the aforementioned reactions and that importantly the chemical treatment of a liquid metal has profound implications on its applicability as a catalyst.

Given that liquid galinstan when immersed in solution would not have a high surface area and therefore unlikely to be particularly active, it was sonicated prior to any test of catalytic activity. It should be noted that the sonication of liquid galinstan into microdroplets has previously been demonstrated.^{8,10} In this process the large galinstan drop is continuously broken apart into smaller droplets. To test the catalytic activity of microsized droplets of galinstan the model system of potassium ferricyanide reduction by sodium thiosulphate was investigated. The reaction involved is the following:



and can be conveniently monitored by UV-visible spectroscopy by a reduction in intensity of the absorption peak associated with $[\text{Fe}(\text{CN})_6]^{3-}$ ions typically observed at 420 nm (Fig. 1). Interestingly, when galinstan was dispersed in water by sonication as in previous studies,^{10a} it was observed that the reaction was very slow and only marginally better than the reaction in the absence of the catalyst. It should be noted that the reaction is thermodynamically favourable but kinetically limited and therefore requires the presence of a catalyst. Given that galinstan

^a School of Chemistry, Physics and Mechanical Engineering, Queensland University of Technology, GPO Box 2434, Brisbane, QLD 4001, Australia.

E-mail: anthony.omullane@qut.edu.au

^b School of Electrical and Computer Engineering, RMIT University, GPO Box 2476, Melbourne, VIC 3001, Australia

† Electronic supplementary information (ESI) available: Full experimental details, UV-vis spectrum of the optimal basic catalyst, FESEM and EDX mapping of the catalyst in 0.1 M NaOH, $\text{In}(A_t/A_0)$ versus time of reduction of $[\text{Fe}(\text{CN})_6]^{3-}$ in the presence of GaCl_3 based catalyst, FESEM and EDX profile of the catalyst in 0.1 M sodium borohydride, time dependant UV-vis absorption spectra of the reduction of potassium dichromate in the presence of galinstan based catalyst, FESEM and EDX profile of the catalyst in 0.1 M formic acid. See DOI: 10.1039/c5cc05246g



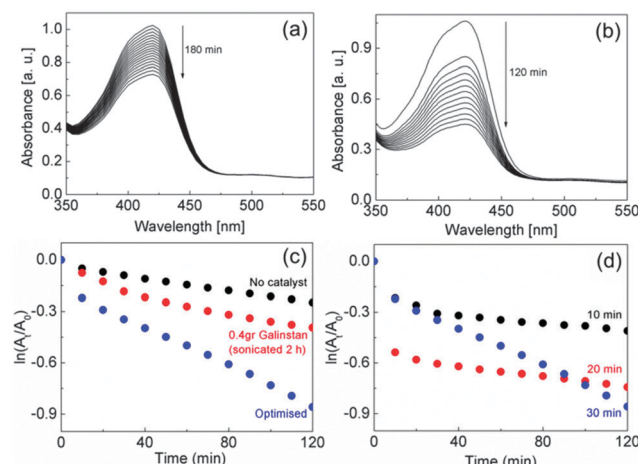


Fig. 1 Time dependant UV-vis absorption spectra of the reduction of 1 mM $[\text{Fe}(\text{CN})_6]^{3-}$ in 0.1 M NaOH in the presence of (a) no catalyst and (b) optimal catalyst, (c) plot of $\ln(A_t/A_0)$ versus time for conditions with no catalyst and a higher loading of catalyst with longer sonication time compared to the optimised catalyst, (d) plot of $\ln(A_t/A_0)$ versus time for different sonication times.

forms a native oxide on the surface at neutral pH, suggests that this oxide impedes the electron transfer process.

Therefore galinstan was sonicated in a 0.1 M NaOH solution to remove this oxide which is mainly comprised of Ga_2O_3 .¹⁶ The catalytic activity increased dramatically and the peak associated with $[\text{Fe}(\text{CN})_6]^{3-}$ decreased in intensity by 58% in 2 h. A UV-vis spectrum of the sonicated galinstan revealed absorption in the UV region and therefore does not contribute in any way to the response in the visible region (Fig. S1, ESI†). The catalytic reaction is assumed to be first order as an excess of thiosulphate is used and therefore a plot of $\ln(A_t/A_0)$ versus Time, where A_t is the absorbance at time t and A_0 is the absorbance at time zero, allows one to determine the reaction rate by calculating the slope of the linear part of the graph. This gave a value of $6.2 \times 10^{-3} \text{ min}^{-1}$ in the presence of the catalyst material which is comparable to Pt nanoparticles ($2.54 \times 10^{-3} \text{ min}^{-1}$).¹⁷ However it is important to note that these are apparent reaction rates and are subject to the conditions employed.¹⁸ Indeed the reaction was undertaken in the presence of 0.1 M NaOH to negate the possibility of oxide formation with time that would otherwise inhibit the reaction (Fig. 1(a)) which differs to previous studies carried out at neutral pH. The mass and sonication time were then optimised for this reaction and it was found that injection of 1 mg of catalyst into the reaction solution gave the best result (Fig. 1(b)). This was achieved by sonicating 300 mg of galinstan in 5 ml of 0.1 M NaOH for 30 min. The required volume of catalyst was then injected into the relevant reactant solution to give a final weight of less than 1 mg of the catalyst. It can be seen from Fig. 1(c) that sonicating a larger amount of galinstan for a longer time did not improve the reaction rate and that sonicating for 30 min gave the optimum result (Fig. 1(d)).

The morphology of the galinstan droplets was investigated with SEM when galinstan was sonicated in water and in 0.1 M NaOH. In water plate-like agglomerates are formed with a rough

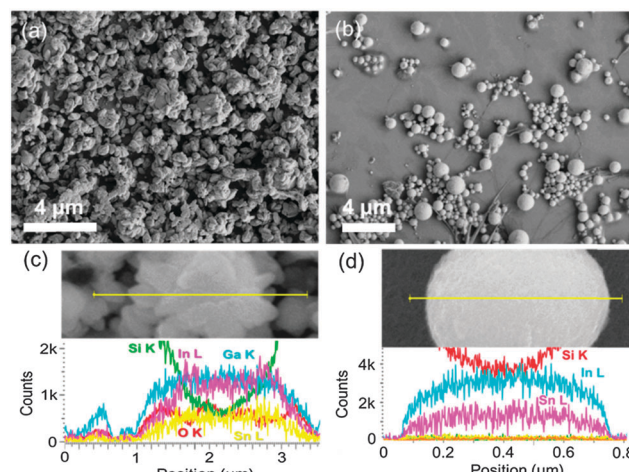
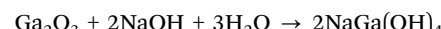


Fig. 2 FESEM images and EDX profiles across the microstructures shown in the high resolution SEM image of galinstan based catalyst after sonication in (a and c) DIW and (b and d) 0.1 M NaOH for 30 min.

texture (Fig. 2(a)) whereas in 0.1 M NaOH smooth sub-micron spheres of different sizes are formed (Fig. 2(b)). Higher magnification images show that the galinstan sonicated in water (Fig. 2(c)) consists of agglomerated small structures that are not spherical as expected for a liquid and is attributed to significant oxidation of galinstan.^{10a} The spherical structures obtained in 0.1 M NaOH are exceptionally uniform (Fig. 2(d)) and show some evidence of nanosized features on the surface.

However, the EDX profiles across the single microstructures shown in the high resolution SEM images revealed an interesting result. While the composition of galinstan was as expected after sonication in water (Fig. 2(c)) (Ga:In:Sn in a 6.9:2.1:1 ratio), this was not the case after sonication in alkaline solution and, a significantly reduced concentration of gallium metal was detected (typically around 6%) whereas the indium to tin ratio of 2 to 1 was preserved (Fig. 2(d)) indicating that Ga metal dissolves in NaOH solution. Therefore when the oxide is removed *via* the action of NaOH the Ga metal continues to be dissolved as fresh galinstan is continuously being generated and oxidised during the sonication procedure. This process occurs until the majority of the gallium core feedstock is consumed and can be represented as:



This hypothesis was confirmed electrochemically at a galinstan microdroplet modified electrode prepared by drop casting the galinstan dispersion in water onto an ITO electrode. The galinstan/ITO electrode was immersed into 0.1 M NaOH and an open circuit potential (OCP) *versus* time experiment was carried out (Fig. 3). The experiment was run for 30 min to be consistent with the sonication time used in the preparation of the catalyst. The experiment was started prior to immersion of the electrode to capture the first contact of galinstan with 0.1 M NaOH. After the initial spike due to charging of the interface there is a rapid decrease in the OCP from 0.96 to -0.24 V which is consistent

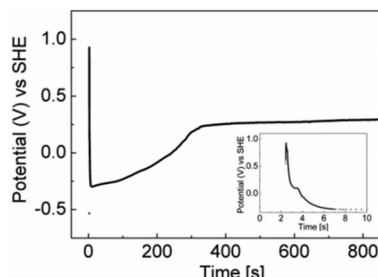


Fig. 3 OCP vs. time recorded in 0.1 M NaOH with galinstan immobilised on ITO as a working electrode (inset: OCP versus time for the first 10 seconds).

with the dissolution of an oxide from a metal surface. This occurs within 10 s after which there is a gradual increase in the OCP value from -0.24 to $+0.21$ V after 350 s. The OCP then remains at an almost constant potential for the remainder of the experiment. The increase in OCP value is consistent with a leaching process. The standard reduction potentials of $\text{Ga}^{3+}/\text{Ga}^0$, $\text{In}^{3+}/\text{In}^0$ and $\text{Sn}^{2+}/\text{Sn}^0$ are -0.529 , -0.340 and -0.138 V vs. SHE respectively. Therefore as Ga metal is dissolved the OCP value is expected to increase and then reach a steady state once it has all been removed and therefore the data suggests this occurs after *ca.* 5 min (for an immobilized film of galinstan, the situation is expected to be even more rapid under sonication conditions).

This raises the possibility that the reaction may in fact be a homogeneous reaction catalysed by the presence of soluble sodium gallate (*i.e.* NaGa(OH)_4) (see Fig. S2 (ESI[†]) for a FESEM image with EDX mapping indicating the formation of this species after dropcasting the catalyst solution onto a surface). Therefore sodium gallate was prepared (see Experimental) and 0.1 ml of this solution was added to the reaction solution and the catalytic performance was studied by UV-vis spectroscopy. Fig. S3 (ESI[†]) shows that the reaction in the presence of NaGa(OH)_4 is significantly slower than that presented in Fig. 2 and hence rules out this possibility. Therefore the catalytic activity originated from the spherical particles that are left consisting of Ga:In:Sn in a 1:10:5 ratio. From this it can be seen that the original In:Sn ratio of 2:1 is preserved and that it is the Ga which is significantly affected by this procedure. From the EDX line scan, In and Sn are evenly distributed across the particles suggesting that an alloy is maintained as in the original galinstan sample. It is interesting that upon the removal of Ga, which is required for galinstan to be a liquid at room temperature, a near perfect spherical shape is maintained even though it cannot be a liquid after such extensive Ga removal. This is most likely due to the system attaining the lowest energy configuration as seen in metal nanoparticle synthesis. In the absence of growth directing agents, nanomaterials tend in the majority of cases to adopt the lowest energy configuration of a sphere. Therefore as galinstan loses its properties as a liquid the resultant solidifying material collapses into solid spherical particles of different sizes consisting mostly of In and Sn with residual Ga.

This material was investigated further for its applicability in more useful catalytic reactions such as 4-nitrophenol reduction

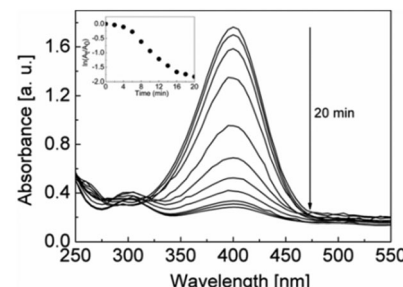


Fig. 4 Time dependant UV-vis absorption spectra of the reduction of 4-nitrophenol in the presence of galinstan based catalyst (inset: plot of $\ln(A_t/A_0)$ versus time).

by sodium borohydride (Fig. 4). This reaction is of interest to the pharmaceutical industry as the aminophenol product is used for the production of analgesic and antipyretic drugs.¹⁹ On these occasions galinstan sonicated in water only was used as the catalyst material. It can be seen in Fig. 4 that the material is catalytically active and gives a rate constant of 0.107 min^{-1} for the conversion of 4-nitrophenol to 4-aminophenol (the absorption band at 300 nm indicates the formation of 4-aminophenol).^{19,20} Given that NaBH_4 is a strong reducing agent it was investigated whether, similar to sodium hydroxide, it modifies the composition of galinstan during the reaction in this case rather than prior to catalysis as in the case of ferricyanide reduction. Therefore in a control experiment the catalyst was kept in 0.1 M NaBH_4 for 180 min and subsequently studied by SEM and EDX and the results are summarised in Fig. S4 (ESI[†]). It can be seen that the gallium concentration is also significantly reduced when galinstan is treated with sodium borohydride (Ga reduced to 3%). Additionally in this case there is also an even distribution of In and Sn across the materials which are again spherical in nature. This would therefore explain the induction time seen for the reaction over the first 4 min (inset of Fig. 4) where the removal of Ga occurs to generate the catalytically active In:Sn spheres (Fig. S4, ESI[†]). This is analogous to the phenomenon often encountered with noble metal nanoparticles such as Au and Pt which also demonstrate an induction time for this reaction due to surface restructuring effects that generates the active material²¹ which can also be in the timescale of minutes.²² Therefore the removal of Ga *via* NaOH or NaBH_4 always results in significant removal of Ga metal from galinstan to give an active In:Sn material.

This implies that this In:Sn rich material with a trace of Ga is quite versatile and that it is not only effective for simpler charge transfer reactions such as the reduction of ferricyanide ions where the surface facilitates the electron transfer process^{15a,23} but also reactions that require a chemical step. The reduction of nitrophenol to aminophenol requires a 6 electron transfer process followed by a hydrogenation process. Even though this reaction is thermodynamically viable when the standard reduction potentials for 4-nitrophenol/4-aminophenol (-0.76 V vs. SHE) and $\text{H}_3\text{BO}_3/\text{BH}_4^-$ (-1.33 V vs. SHE) are considered, the reaction still requires a catalyst as in its absence there was no change in the intensity of the peak at 400 nm after 3 hours. Once nitrophenolate ions are adsorbed on the surface (generated from nitrophenol in the

presence of NaBH_4 as indicated by the peak at 400 nm in Fig. 4), electron transfer is initiated from the borohydride ions into the catalyst and hydrogenation of the nitro group occurs followed by desorption of the product.^{11a,15b,18,20,21,24}

Therefore, it appears that the catalytic activity of the modified material is governed by its composition. To support this hypothesis, the material was used as a catalyst in the reduction of potassium dichromate by formic acid (Fig. S5, ESI[†]). It was found that when galinstan was kept in formic acid for 180 min, In and Sn were homogeneously dispersed within the material (Fig. S6, ESI[†]) with a gallium concentration as high as 44% which is much larger compared to the cases where NaOH or NaBH_4 were used for the previous reactions. For this catalytic reaction the peak associated with the dichromate ion at 350 nm decreased in intensity by 15% after 2 h to give a rate of $1.1 \times 10^{-3} \text{ min}^{-1}$ indicating that this material is not particularly active towards this reaction. Therefore, it suggests that the amount of Ga that is present in the final composition dictates the catalytic activity.

In summary, we demonstrated the design and synthesis of a widely applicable new material based on solid microspheres generated from a liquid galinstan precursor. Significantly, galinstan dispersed in an alkaline solution or when treated with a strong reducing agent such as NaBH_4 removes Ga metal to give solid spherical micron sized catalyst particles with an In : Sn ratio of 2 : 1 with a reduced Ga content. This material is highly effective towards the reduction of ferricyanide and nitrophenol. This work illustrates the interesting chemical properties of galinstan in liquid media and may also lead to enhanced application of this material in organic transformation reactions.

AOM gratefully acknowledges funding through a Future Fellowship from the Australian Research Council (FT110100760). The data reported in this paper were obtained at the *Central Analytical Research Facility* operated by the *Institute for Future Environments* (QUT). Access to CARF is supported by generous funding from the Science and Engineering Faculty (QUT).

Notes and references

1 (a) H.-J. Koo, J.-H. So, M. D. Dickey and O. D. Velev, *Adv. Mater.*, 2011, **23**, 3559; (b) J.-H. So, H.-J. Koo, M. D. Dickey and O. D. Velev, *Adv. Funct. Mater.*, 2012, **22**, 625; (c) B. J. Blaiszik, S. L. B. Kramer, M. E. Grady, D. A. McIlroy, J. S. Moore, N. R. Sottos and S. R. White, *Adv. Mater.*, 2012, **24**, 398.

- 2 S.-Y. Tang, K. Khoshmanesh, V. Sivan, P. Petersen, A. P. O'Mullane, D. Abbott, A. Mitchell and K. Kalantar-zadeh, *Proc. Natl. Acad. Sci. U. S. A.*, 2014, **111**, 3304.
- 3 S. Cheng and Z. Wu, *Adv. Funct. Mater.*, 2011, **21**, 2282.
- 4 M. Hodes, Z. Rui, L. S. Lam, R. Wilcoxon and N. Lower, *IEEE Trans. Compon., Packag., Manuf. Technol.*, 2014, **4**, 46.
- 5 M. G. Blaber, C. J. Engel, S. R. C. Vivekchand, S. M. Lubin, T. W. Odom and G. C. Schatz, *Nano Lett.*, 2012, **12**, 5275.
- 6 (a) V. Sivan, S.-Y. Tang, A. P. O'Mullane, P. Petersen, N. Eshtiaghi, K. Kalantar-zadeh and A. Mitchell, *Adv. Funct. Mater.*, 2013, **23**, 144; (b) P. Surmann and H. Channaa, *Electroanalysis*, 2015, **27**, 1726.
- 7 T. Krupenkin and J. A. Taylor, *Nat. Commun.*, 2011, **2**, 448.
- 8 (a) J. W. Boley, E. L. White and R. K. Kramer, *Adv. Mater.*, 2015, **27**, 2355; (b) J. N. Hohman, M. Kim, G. A. Wadsworth, H. R. Bednar, J. Jiang, M. A. LeThai and P. S. Weiss, *Nano Lett.*, 2011, **11**, 5104.
- 9 (a) S.-Y. Tang, V. Sivan, K. Khoshmanesh, A. P. O'Mullane, X. Tang, B. Gol, N. Eshtiaghi, F. Lieder, P. Petersen, A. Mitchell and K. Kalantar-zadeh, *Nanoscale*, 2013, **5**, 5949; (b) V. Sivan, S.-Y. Tang, A. P. O'Mullane, P. Petersen, K. Kalantar-zadeh, K. Khoshmanesh and A. Mitchell, *Appl. Phys. Lett.*, 2014, **105**, 121607.
- 10 (a) W. Zhang, J. Z. Ou, S.-Y. Tang, V. Sivan, D. D. Yao, K. Latham, K. Khoshmanesh, A. Mitchell, A. P. O'Mullane and K. Kalantar-zadeh, *Adv. Funct. Mater.*, 2014, **24**, 3799; (b) W. Zhang, B. S. Naidu, J. Z. Ou, A. P. O'Mullane, A. F. Chrimes, B. J. Carey, Y. Wang, S.-Y. Tang, V. Sivan, A. Mitchell, S. K. Bhargava and K. Kalantar-zadeh, *ACS Appl. Mater. Interfaces*, 2015, **7**, 1943.
- 11 (a) P. Herves, M. Perez-Lorenzo, L. M. Liz-Marzan, J. Dzubiella, Y. Lu and M. Ballauff, *Chem. Soc. Rev.*, 2012, **41**, 5577; (b) A. Vojvodic and J. K. Nørskov, *Nat. Sci. Rev.*, 2015, **2**, 140; (c) E. Gross, F. Dean Toste and G. Somorjai, *Catal. Lett.*, 2015, **145**, 126.
- 12 (a) W. Yu, M. D. Porosoff and J. G. Chen, *Chem. Rev.*, 2012, **112**, 5780; (b) M. Sankar, N. Dimitratos, P. J. Miedziak, P. P. Wells, C. J. Kiely and G. J. Hutchings, *Chem. Soc. Rev.*, 2012, **41**, 8099; (c) A. Villa, D. Wang, D. S. Su and L. Prati, *Catal. Sci. Technol.*, 2015, **5**, 55.
- 13 Z. Zhang, C. Shao, Y. Sun, J. Mu, M. Zhang, P. Zhang, Z. Guo, P. Liang, C. Wang and Y. Liu, *J. Mater. Chem.*, 2012, **22**, 1387.
- 14 A. Dandapat, D. Jana and G. De, *Appl. Catal., A*, 2011, **396**, 34.
- 15 (a) I. Najdovski, P. R. Selvakannan and A. P. O'Mullane, *RSC Adv.*, 2014, **4**, 7207; (b) I. Najdovski, P. R. Selvakannan, S. K. Bhargava and A. P. O'Mullane, *Nanoscale*, 2012, **4**, 6298.
- 16 P. Sipos, T. Megyes and O. Berkesi, *J. Solution Chem.*, 2008, **37**, 1411.
- 17 Y. Li, J. Petroski and M. A. El-Sayed, *J. Phys. Chem. B*, 2000, **104**, 10956.
- 18 D. Jana, A. Dandapat and G. De, *Langmuir*, 2010, **26**, 12177.
- 19 Y. Lu, J. Yuan, F. Polzer, M. Drechsler and J. Preussner, *ACS Nano*, 2010, **4**, 7078.
- 20 F.-h. Lin and R.-a. Doong, *J. Phys. Chem. C*, 2011, **115**, 6591.
- 21 S. Wunder, F. Polzer, Y. Lu, Y. Mei and M. Ballauff, *J. Phys. Chem. C*, 2010, **114**, 8814.
- 22 X. Zhou, W. Xu, G. Liu, D. Panda and P. Chen, *J. Am. Chem. Soc.*, 2010, **132**, 138.
- 23 (a) D. Li, C. Sun, Y. Huang, J. Li and S. Chen, *Sci. China, Ser. B: Chem.*, 2005, **48**, 424; (b) P. L. Freund and M. Spiro, *J. Chem. Soc., Faraday Trans.*, 1986, **1**, 82.
- 24 H. Liu and Q. Yang, *J. Mater. Chem.*, 2011, **21**, 11961.

